UDC 537.61:681.327.634

# Advanced Stiction-Free Slider and DLC Overcoat

●Takayuki Yamamoto ●Yoshiharu Kasamatsu ●Hiroyuki Hyodo

*(Manuscript received September 17, 2001)*

**The demand for higher areal densities in hard disks requires a lowering of the magnetic spacing between heads and media. To achieve this, the flying height of the slider and the thickness of the slider and media overcoats must be lowered.**
**To fly a slider stably at low altitude, the media surface must be as smooth as possible. However, some degree of surface roughness is beneficial because it keeps the head from adhering to the disk when at rest. Reducing the contact area between the head and disk is the most suitable way of lowering the stiction force. This can be achieved by adding contact pads to the air-bearing surface, resulting in what we call a stiction free slider (SFS). On the other hand, overcoat thickness must be reduced while maintaining the durability and anti-corrosion properties. In this paper, we first focus on the material and tribological properties of sputtered hydrogenated amorphous carbon films, which are currently used for the overcoats of thin film media. Then, we describe the PCVD technique for the next generation of overcoats. Finally, we describe a tetrahedral amorphous carbon overcoat deposited by filtered cathodic arc deposition, which will be used in the future.**

## 1. Introduction

In the 1990s the areal recording density of hard disk drives (HDDs) grew at the remarkable rates of 60% to 100% per year, and it is expected to increase further in the 21st century. Magnetic devices such as giant magnetoresistive effect (GMR) heads and low-noise thin film magnetic media, mechatronics, and signal processing technologies have been improved, but the principle of magnetic recording necessitates the reduction of spacing between heads and media to increase the areal recording density. The size of the magnetic spacing is the flying height of the head plus the thickness of the head and media overcoats. There are many head-disk interface technologies to secure stable flying at a low fly height; however, we focused on the SFS and the overcoat for thin film media.

To fly a head safely at a low flying height, the surface roughness of the disk must be lowered, but this also increases the stiction force. To reduce the stiction force, sophisticated texturing schemes have been employed to introduce topography on the disk in a highly controlled manner. However, the conventional CSS (Contact Start Stop) method, which is the combination of a slider with a crown shaped ABS (Air Bearing Surface) and a mechanical textured disk surface, cannot prevent a high stiction force, which can result in a disk spin-up failure. Alternatives to the conventional CSS method are laser zone texturing,[1] a ramp load technology,[2] and a padded slider.[3),4] Fujitsu has developed a padded slider, called a stiction free slider (SFS), and has applied it to all HDD products since the fall of 1997.

The overcoat thickness of the slider and disk surface is currently around 6 nm. Nitrogenated and hydrogenated amorphous carbon films (a-C:N or a-C:H) made by DC magnetron sputtering have been widely used as the overcoats for

disks, because of their superior tribology and corrosion resistance.[5] However, the thickness of overcoats must be further reduced while maintaining their durability and anti-corrosion properties. Therefore, plasma chemical vapor deposition (pCVD) and ion beam deposition (IBD) have recently been applied as alternatives to sputtering deposition because of the higher hardness and coverage of the films they create.[6)–8)]

However, within a few years, the thickness of overcoats is expected to be around several nanometers, and it is not clear if these films will continue to provide their excellent performance. Filtered cathodic arc (FCA) deposition shows higher wear resistance and high anti-corrosion properties, and it will probably be the next-generation deposition technique for an ultra thin disk overcoat.

This paper reviews our state-of-the-art stiction free slider and diamond-like carbon (DLC) overcoat technologies for sliders and disks.

## 2. Stiction free slider

### 2.1 Stiction phenomena

The stiction of the head-disk interface can be modeled in terms of the effect of the menisci of the liquid between the slider and disk surfaces. Mamine et al. proposed that there are two distinct regimes of stiction behavior: the flooded regime and the toe-dipping regime. These two regimes are characterized by differing levels of "fill" in the interface and so depend on the mean separation, $h$, and the liquid film thickness, $t$. The flooded regime occurs when $t > h$, and the toe-dipping regime occurs when $t < h$.[9)]

In the toe-dipping regime, the stiction force $F$ is given by:

$$F = N^{*}4\pi R\,\gamma\cos\theta \qquad (1),$$

where $N$ is the number of liquid mediated asperities between slider and disk, $R$ is the curvature of asperity, $\gamma$ is the surface tension of the liquid, and $\theta$ is the contact angle of the liquid to the slider and disk surface. In the flooded regime, the force is given by:

$$F = S\,\gamma\cos\theta / h \qquad (2),$$

where $S$ is the area of the liquid junction between the slider and disk. Liu et al. proposed another region called the excessive lube regime.[10)] In this region, the stiction force is given by:

$$F = S\,\gamma\cos\theta / r \qquad (3),$$

where $r$ is the radius of curvature of the liquid's meniscus.

In the toe-dipping regime, $N$ is inversely proportional to the surface roughness and proportional to the thickness of the liquid (i.e., lubricant).[11),12)] Therefore, the stiction force is proportional to $d/Ra$, where $d$ is the thickness of lubricant and $Ra$ is the average roughness of the disk. In the flooded regime, $h$ depends on the roughness of the disk and the stiction force is higher than the stiction force in the toe-dipping regime. The geometric considerations show that $r$ is proportional to the lubricant thickness. In the excessive lube regime, the stiction force decreases with the lubricant thickness. Our experimental results shown in **Figure 1** agree with these theoretical considerations.

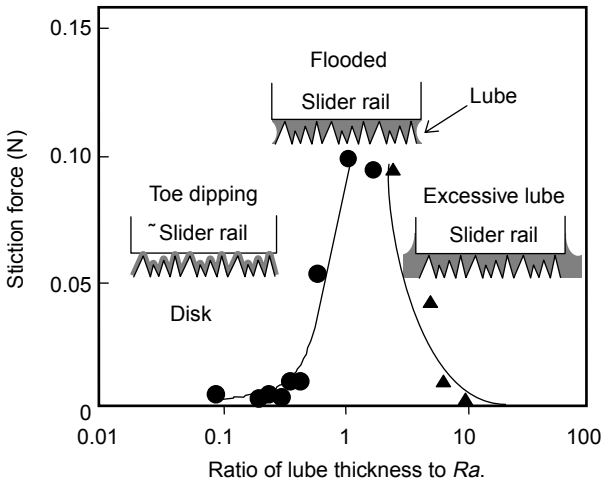


Figure 1
Stiction regime.

## 2.2 Stiction free slider (SFS)

The SFS has four oval pads on the air bearing surface (ABS), as shown in **Figure 2**. These pads are made of DLC and are formed by a photolithography technique. **Figure 3** shows the SFS fabrication process. Si (adhesion layer), DLC (ABS overcoat), Si (etching stopper layer), and DLC (pad layer) films are sequentially deposited onto an $Al_2O_3TiC$ bar that is cut from a wafer after a Read/Write element process. In this study, DLC films were deposited by electron cyclotron resonance-chemical vapor deposition (ECR-CVD) and Si films were deposited by sputtering. A photoresist film was coated onto the DLC film (Figure 3 (a)) and the surface was irradiated with ultraviolet (UV) light through a photomask of the pad pattern (Figure 3 (b)). The non-irradiated photoresist was dissolved in a development step to form the mask pattern. The DLC and Si films without the resist mask pattern were removed by reactive ion etching (RIE) of $O_2$ and $CF_4$, respectively (Figure 3 (c)). Pad fabrication was completed by removing the irradiated resist with acetone (Figure 3 (d)). Finally, the ABS was fabricated into a Guppy with no crown.[13)]

**Figure 4** shows the stiction force as a function of the pad area for disks with *Ra* = 1.2 nm and a 2.0 nm thick lubricant. The stiction force seems to increase linearly with the pad area. The stiction force was caused by a meniscus force induced via liquid mediated contact between the two surfaces in the toe-dipping regime. The number of liquid mediated contacts between the pads and disk is assumed to be proportional to the pad area. **Figure 5** shows the stiction force versus pad

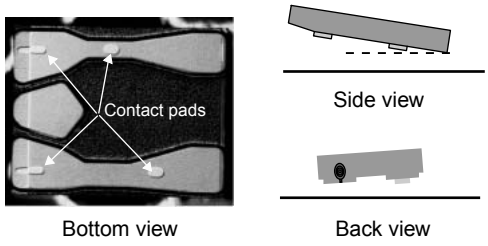


Figure 2
Stiction free slider.

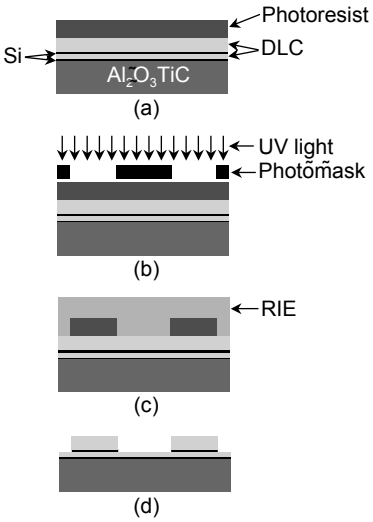


Figure 3
SFS fabrication process.

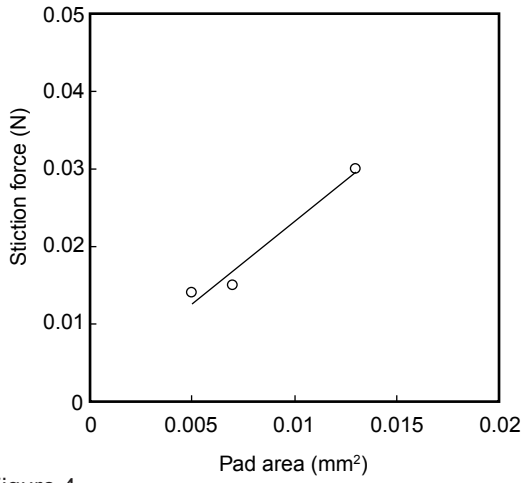


Figure 4
Pad area vs. stiction force.

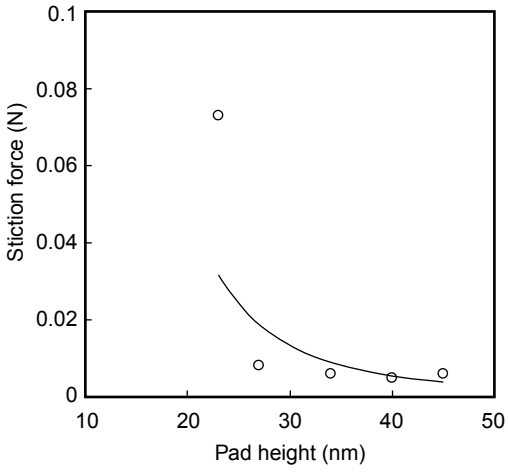


Figure 5
Pad height vs. stiction force.

height for a pad area of 0.009 mm$^2$, disks with a 2.8 nm *Ra*, and a 1.5 nm thick lubricant. The stiction force increases sharply when the pad is below a critical height of about 25 nm. This stiction force avalanche is explained by the following model.[14),15)] When the pads rest on the disk, lubricant redistribution has to occur in order to maintain equilibrium between the capillary pressure inside the menisci and the disjoining pressure of the lubricant film outside the menisci. The liquid lubricant film is drawn from the surrounding area to join the menisci. In this case, the meniscus height of equilibrium is 25 nm when the Hamaker constant is assumed to be $1.5 \times 10^{-9}$ J. If the pad height is lower than the menisci height at the equilibrium point, the lubricant fills the gap between the ABS and disk and the stiction force increases drastically.

The pad wear after 100 000 CSS cycles as a function of the surface roughness is shown in **Figure 6**. The pad area was 0.009 mm$^2$ and the lubricant thickness was 2 nm. The pad wear increased slightly with the surface roughness, but is negligible. We have confirmed that the wear of a pad area of 0.003 mm$^2$ was also negligible. These good results were achieved by lowering the applied load,[16)] optimizing the deposition conditions of DLC films for pads,[17)] and specially tailoring the disk surface. After 100 000 CSS cycles, there was no visible wear on the disk surface. Consequently, we can conclude that the SFS pads are durable enough for practical use.

**Figure 7** shows the stiction force versus surface roughness of a disk with a lubricant thickness of 2 nm and pad areas of 0.003 and 0.009 mm$^2$. In the case of the SFS with a pad area of 0.009 mm$^2$, reducing *Ra* down to 0.7 nm does not affect the stiction force. However, when *Ra* reaches 0.5 nm, the stiction force begins to rise sharply. In the case of the SFS with a pad area of 0.003 mm$^2$, even when *Ra* is reduced to 0.25 nm there is only a small increase in stiction force. These results are accurately simulated using Li and Talke's model.[11)]

The SFS shows an excellent CSS performance on a surface roughness of 0.3 nm, which provide the flattest possible artificial surface. Therefore, we can conclude that SFSs have a high potential to reduce the stiction force on the smooth surface of disks.

## 2.3 Advanced stiction free slider

The spindle motor in an HDD rotates backward just before it completely stops. When a disk is ro-

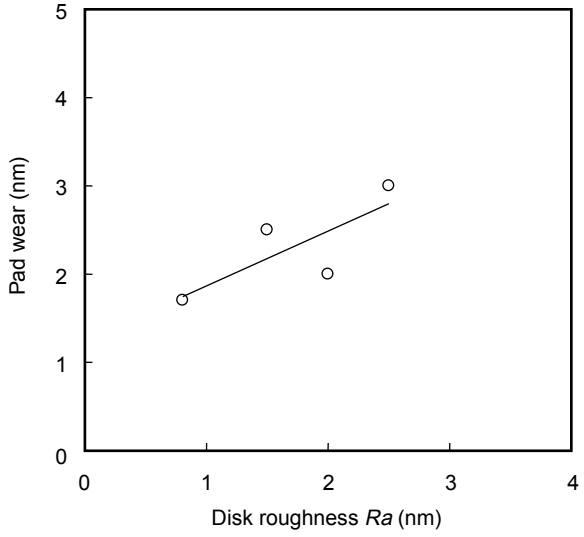


Figure 6
Surface roughness vs. pad wear.

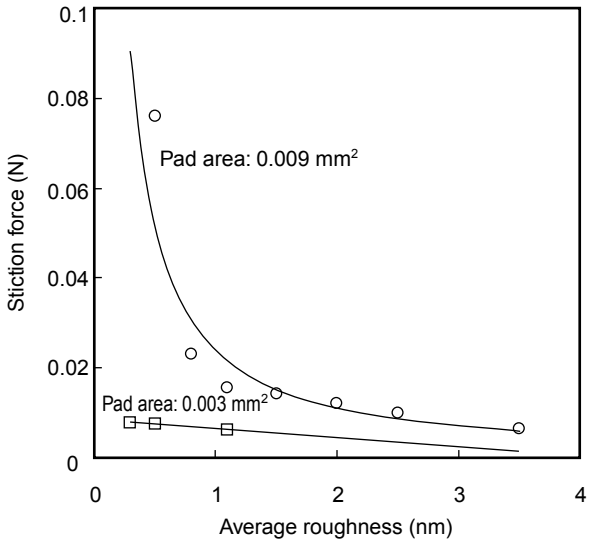


Figure 7
Surface roughness vs. stiction force.

tated backward, the slider tips backward so that the trailing edge area contacts the disk. A large, low-profile meniscus could form in this area and cause excessive stiction as shown in **Figure 8 (a)**. A quick estimation using a model of the flooded regime suggests that the maximum stiction force could exceed 9 gf. To prevent spreading lubricant over the area on the trailing edge, a shallow groove was fabricated near the edge as shown in **Figure 8 (b)**.

The effect of the groove was experimentally examined by measuring the stiction force after rotating the spindle backward. SFSs with 6 nm-depth-grooves were selected for controlled tipping tests on a lightly textured media lubed to a thickness of 0.8 to 1.6 nm. The test results are shown in **Figure 9**. For the SFSs without grooves, the stiction force after backward rotation increased with the lubricant thickness. However, the stiction force for the grooved SFSs remained low even with the thicker layer of lubricant.

We applied the grooved SFS technology to a new ABS for ultra low flying heights as shown in **Figure 10**.[18] The advanced SFS technology allows the CSS solution to be extended to the head-disk interface as a prominent alternative to the ramp road technology, thereby breaking the stiction barrier on an ultra smooth disk for over 100 Gbit/in$^2$ recording.

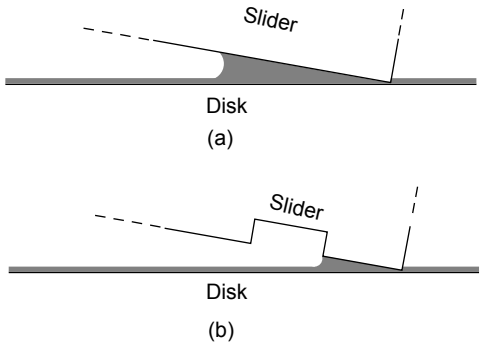


Figure 8
Head tipping.

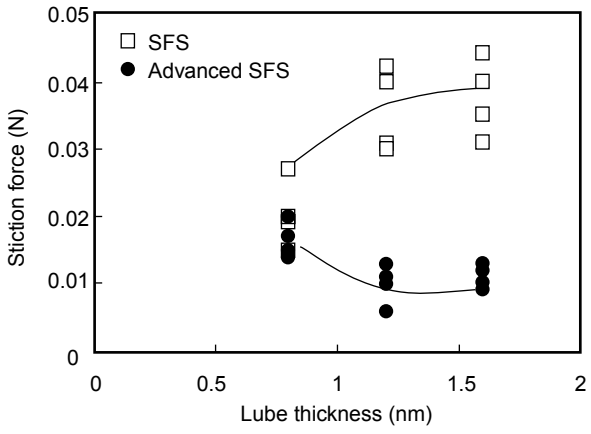


Figure 9
Lube thickness vs. stiction force.

## 3. DLC overcoat

### 3.1 Sputtered DLC overcoat

Today, all rigid disks are made using thin-film technology, particularly the sputtering process. A magnetic film sputtered on a smooth surface cannot withstand friction, wear, and corrosion by itself. Several materials other than amorphous carbon films, $SiO_2$, and $ZrO_2$ have been studied and used for the overcoats of thin film disks.[19),20)] However, sputtered amorphous carbon films have recently been applied to thin-film media in general because sputtered amorphous carbon films and magnetic films can be deposited successively by the sputtering process and display superior tribological and anti-corrosion properties.[21),22)]

Figure 10
Advanced SFS.

The a-C film is usually deposited by DC magnetron sputtering using a graphite target in pure argon gas. The a-C:H and a-C:N film are deposited by reactive sputtering using a graphite target in a mixture of argon and hydrogen/methane or in pure nitrogen. Incorporating hydrogen or nitrogen into amorphous carbon film hardens the film, thus increasing its durability. Typical Raman spectra of a-C, a-C:N, and a-C:H are shown in **Figure 11**. The main features of these spectra are the D and G bands characteristic of all amorphous carbon forms. The bands can be analyzed quantitatively using a computer program to reproduce the data as the sum of two combinations of Gaussian and Lorentzian lines.[23] The position $\Gamma_i$, the line width $\omega_i$, and the intensity for each line are used as fitting parameters. The values for the parameters obtained in the Raman analyses are listed in **Table 1**. A decrease in the Id/Ig ratio and the downshifted D and G line position was observed as nitrogen or hydrogen was incorporated into the films. These results suggested that the structural changes were caused by the incorporation of hydrogen or nitrogen.

## 3.2 Plasma CVD DLC overcoat

a-C:H films deposited by pCVD or IBD methods are now being applied to thin-film media as overcoat films. We have been studying an a-C:H film deposited by hot-filament pCVD using toluene as a precursor material.[24] This deposition system consists of two hot-filament cathode electrodes, two anode electrodes, and two bias grids in a stainless steel chamber. The substrate is held outside the plasma, between two bias grids. Hot filament electrodes emit thermal electrons to discharge monomers. The plasma is generated between the cathodes and anodes, and bias grids remove ions from the plasma.

The chamber was first evacuated to a pressure of $1 \times 10^{-3}$ Pa by a turbo-molecular pump. First, the substrate surface was cleaned using hydrogen plasma. Then, toluene ($C_7H_8$) was introduced into the chamber at a pressure of 0.03 Pa. AC power for the cathodes and the DC voltages for the anodes and bias grids were then applied for deposition. The film thickness was controlled by controlling the integrated ion current at each bias grid.

The relationship between the bias voltage and the chemical structure is shown in **Figure 12**. The bias voltage was varied from –250 to –1250 V. The hydrogen content in the film was determined by measuring the amount of carbon-hydrogen bonding using Fourier transform infrared spectroscopy (FTIR).

Id/Ig dramatically decreased at a bias volt-

Table 1
Parameters of Raman spectra in Figure 11.

| | Id/Ig | $\Gamma_D$(cm$^{-1}$) | $\omega_D$(cm$^{-1}$) | $\Gamma_G$(cm$^{-1}$) | $\omega_G$(cm$^{-1}$) |
|---|---|---|---|---|---|
| a-C | 4.6 | 363 | 1394 | 154 | 1569 |
| a-C:N | 3.7 | 364 | 1337 | 175 | 1555 |
| a-C:H | 1.9 | 367 | 1383 | 162 | 1555 |

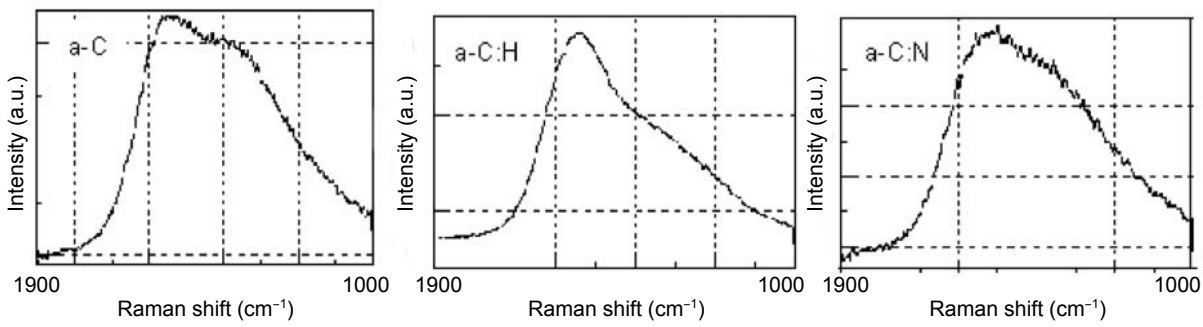


Figure 11
Raman spectra of a-C, a-C:H, and a-C:N.

age of –250 V and –500 V. The hydrogen content in the film decreased as the bias voltage increased. Increasing the substrate bias increased the energy of the precursor ions moving into the substrate surface, increasing the ion bombardment. The increases in ion bombardment induced the formation of $sp^3$-bonded carbon and dehydrogenation in the film. These results suggest that increasing the bias voltage increased the microscopic diamond structure in the film, which in turn increased the hardness of the film.

The increased hardness of the film enhances durability. As shown in **Figure 13**, the durability of the film increased linearly with the film hardness. Durability was measured by a pin on disk tester. The spherical surface of the pins (1 mm surface curvature radius) was made of $Al_2O_3$-TiC ceramic. The sliding speed was 0.3 m/s, and the applied load was 0.1 N. The test was conducted on an 8 nm thick film without lubricant and in ambient atmosphere.

**Figure 14** compares the durabilities of a pCVD film deposited under the most suitable deposition conditions and a sputtered a-C:H film. The durabilities of both films increase with film thickness. The pCVD films displayed a greater durability than the sputtered film, particularly at thicknesses below 8 nm, where there is a marked drop in the durability of the sputtered a-C:H film. The greater durability of the pCVD appears to originate from the increase in hardness. The pCVD film enables us to reduce the overcoat thickness of the magnetic disks and thus reduce magnetic spacing and ensure a higher recording density.

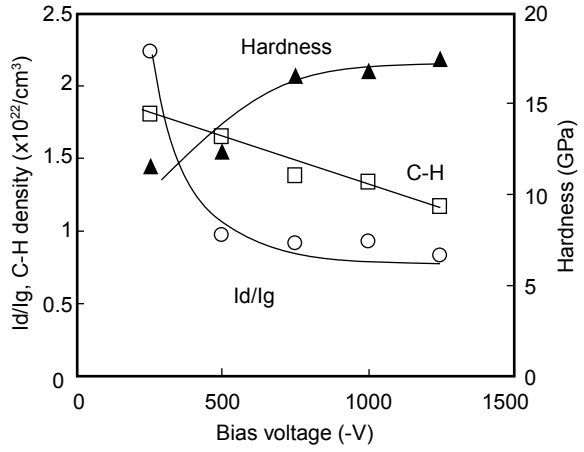


Figure 12
Bias voltages vs. film properties.

## 3.3 Filtered Cathodic Arc Deposition DLC overcoats

The schematic diagram of an FCA deposition system is shown in **Figure 15**.[25] Pure graphite is used for the cathode target. Carbon ions are produced from a cathode spot by arc discharge between the cathode target and anode. Although electrons, macro-particles, and neutrals of carbon

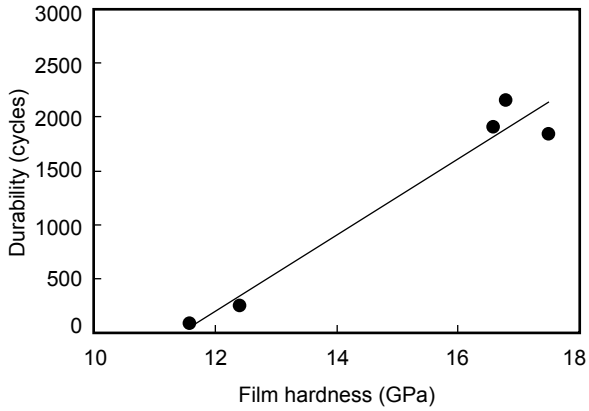


Figure 13
Film hardness vs. durability.

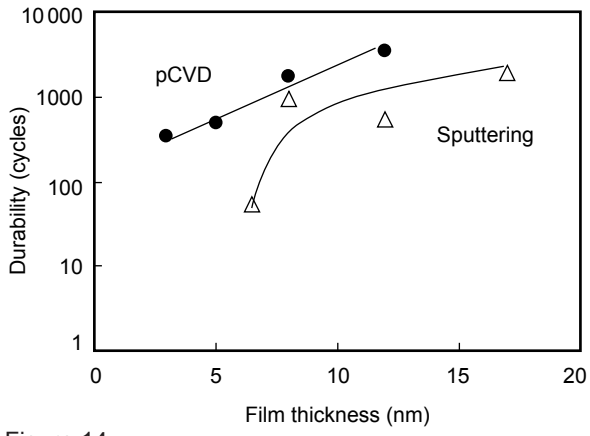


Figure 14
Film thickness vs. durability.

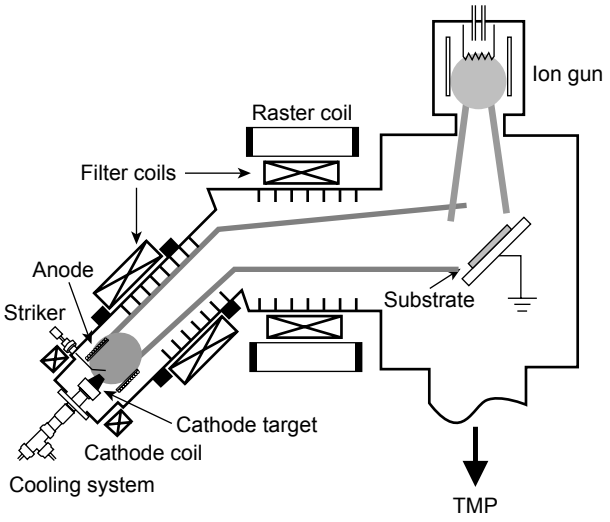


Figure 15
FCA deposition apparatus.

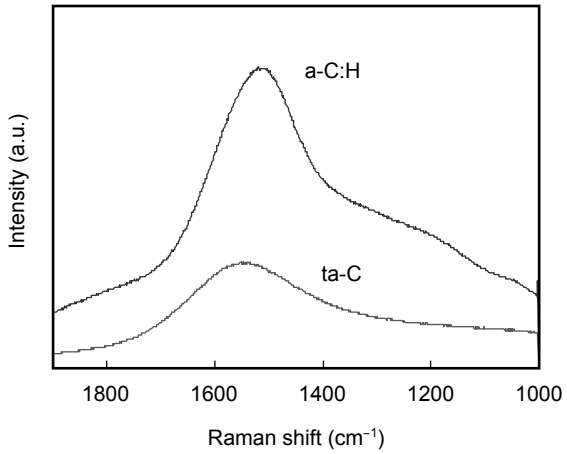


Figure 16
Raman spectra of a C:H and ta-C films.

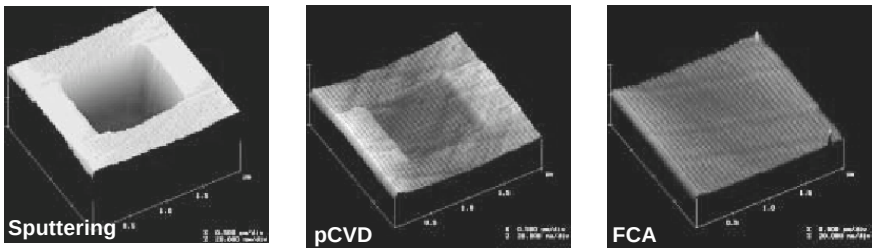


Figure 17
AFM images of nanowear patterns.

are simultaneously produced, a magnetic filter removes the macro-particles and neutrals, so only carbon ions and electrons reach the substrate. The deposition system also has an ion gun which can be used for surface cleaning before deposition and for nitrogen doping into the film.

**Figure 16** shows the Raman spectra of a tetrahedral amorphous carbon (ta-C) film prepared by FCA and an a-C:H film prepared by pCVD. The thickness of these samples is the same. The typical spectrum of an a-C:H film has a G-band peak around 1550 $cm^{-1}$ and a D-band peak around 1350 $cm^{-1}$. The G-band peak is due to the movement of $sp^2$ carbon to the graphite plane, and the D-band peak is due to disorder in the graphite structure. In the ta-C film, the G-band peak intensity is low and no significant D-band peak is observed. The background noise caused by the polymeric structure in the film is also low because FCA deposition is a hydrogen-free process. These results show that the ta-C film contains a large amount of $sp^3$ bonding compared with the a-C:H film. The shapes of the spectra are not changed when the arc current and cathode coil current are varied. The deposition rate increases with arc current. The hardness of these films has been measured at about 26 GPa and it does not show any dependence on the arc current or the cathode coil current.

The nanowear properties were measured using an atomic force microscope (AFM) with a sharp diamond tip. The test was performed at 10 µN using 12 scans over a distance of 10 µm. **Figure 17** shows the results of a nanowear test. The residual depth of the nanowear pattern is 10 nm on the sputtered film and 2 nm on the pCVD

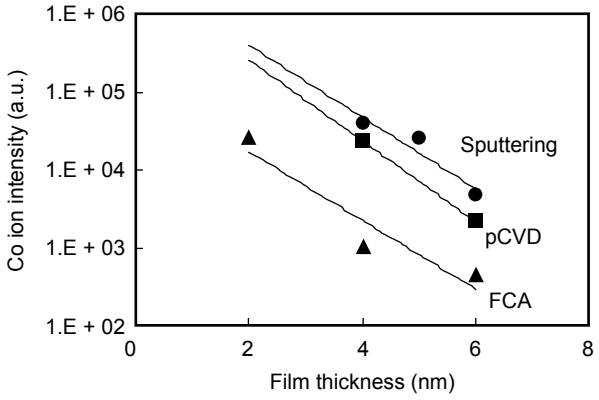


Figure 18
Corrosion resistance of sputtered, pCVD, and FCA carbon films evaluated by TOF-SIMS.

film. However, no nanowear pattern can be observed on the FCA film. This shows that ta-C films have a high wear resistance compared with a-C:H films made by sputtering and pCVD.

The amount of Co ions on the carbon surfaces, which were exposed to hot and humid conditions for several tens of hours, was measured by time of flight secondary ion mass spectroscopy (TOF-SIMS) as shown in **Figure 18**. Cobalt in magnetic recording films migrates through tiny holes, perhaps as small as a few nm in diameter, in the carbon films. These holes allowed an electrochemical corrosion system to be established when moisture was present at the holes, which accelerated the deterioration of the magnetic film. The amount of Co ions increased as the film thickness decreased. However, Co ions on the FCA carbon film were much smaller than those on sputtered and pCVD films. This shows that the anti-corrosion properties of FCA carbon films are superior to those of other films.

FCA carbon films have superior durability and anti-corrosion properties to CVD carbon films and can safely be used in smaller thicknesses to achieve higher recording densities.

## 4. Summary

The areal densities of commercial HDDs will increase at a rate of 100% per year and exceed 100 Gbit/in$^2$ in a few years. In this paper, we presented two state-of-the-art technologies: the advanced stiction free slider (SFS) and the diamond-like carbon (DLC) overcoat.

Advanced SFSs offer excellent control of the apparent head-disk contact area and can reduce the stiction force on ultra smooth disks. Filtered cathodic arc (FCA) DLC overcoats show excellent durability and anti-corrosion properties. These novel techniques have an excellent potential to overcome the tribological obstacles and thus enable ultra-high density recordings.

## References

1) J. J. Liu, W. Liu, and K. E. Jhonson: Current and Future Approaches for Laser Texturing of thin film media. *IEEE Trans. Magn.*, **36**, p.125-132 (2000).
2) Q. Zeng and D. B. Bogy: Effects of certain design Parameters on Load/Unload Performance. *IEEE Trans. Magn.*, **36**, p.140-147 (2000).
3) Y. Kasamatsu, T. Yamamoto, S. Yoneoka, and Y. Mizoshita: Stiction Free Slider for ultra smooth disk. *IEEE Trans. Magn.*, **31**, p.2961-2963 (1995).
4) T. Yamamoto, T. Yokohata, and Y. Kasamatsu: Stiction Free Slider for a lightly textured disk. *IEEE Trans. Magn.*, **34**, p.1783-1785 (1998).
5) T. Yamamoto, T. Toyoguchi, and F. Honda: Ultra thin Amorphous C:H overcoats by pCVD on thin film media. *IEEE Trans. Magn.*, **36**, p.115-119 (2000).
6) B. Marchon, P. N. Vo, and R. Khan: Structure and mechanical properties of hydrogenated carbon films prepared by magnetron sputtering. *IEEE Trans. Magn.*, **27**, p.5160-5163 (1990).
7) T. Toyoguchi, T. Yamamoto, and R. Koishi: Material and Tribological Properties of a-C:H Film by Plasma CVD for a disk overcoat. *IEEE Trans. Magn.*, **34**, p.1741-1743 (1998).
8) K. J. Grannen, X. Ma, R. Thangaraj, J. Gui,

and G. C. Rauch: Ion Beam Deposition of Carbon Overcoats for Magnetic Thin Film Media. *IEEE Trans. Magn.*, **36**, p.120-124 (2000).

9) M. J. Matthewson and H. J. Mamine: Liquid Mediated Adhesion of Ultra-flat Solid Surfaces. Mat. Res.Soc.Symp. Proc. 119, 1988, p.87-92.
10) Z. Liu, E. Rabinowicz, and N. Saka: The Stiction between Magnetic Recording Heads and Thin Film Disks. STLE Special Publication SP-30, p.64-70, 1991.
11) Y. Li and F. Talke: Effect of Humidity on Stiction and Friction of the Head/Disk Interface. *IEEE Trans. Magn.*, p.2487-2489 (1990).
12) H. Tian and T. Matsudaira: Effect of Relative Humidity on Friction Behavior of the Head/Disk Interface. *IEEE Trans. Magn.*, **28**, p.2530-2532 (1992).
13) S. Yoneoka, M. Katayama, T. Ohwe, Y. Mizoshita, and T. Yamada: A Negative Pressure Micro-head Slider for Ultra-low Spacing with Uniform Flying Height. *IEEE Trans. Magn.*, **27**, p.5085-5087 (1991).
14) C. M. Mate and V. J. Novotony: Molecular Conformation and Disjoining Pressure of Polymeric Liquid Films. *J. Chem. Phys.*, **94**, p.8420-8427 (1991).
15) J. Gui and B. Marchon: A Stiction Model for a Head-Disk Interface of a Rigid Disk Drive. *J. Appl. Phys.*, **78**, p.4206-4217 (1955).
16) T. Ohwe, T. Watanabe, S. Yoneoka, and Y. Mizoshita: A New Integrated Suspension for Pico-Sliders (Pico-CAPS). *IEEE Trans. Magn.*, **32**, p.3648-3650 (1996).
17) T. Yamamoto, T. Toyoguchi, and T. Takagi: Chemical and Tribological Properties of Amorphous Hydrogenated Films by ECR-CVD. Poster session at DIAMOND Conf., France, Sept. 1996.
18) R. Koishi, S. Yoneoka, A. Suzuki, Y. Kasamatsu, and Y. Mizoshita: The Trinity Slider for Ultra Low Flying Heights. EP-07 Digests of Intermag Conf., Korea, 1999.
19) M. Yanagisawa: Tribological Properties of Spin-coated SiO2 Film on Plated Magnetic Recording Disks. Tribology and Mechanics of Magnetic Storage Systems, 2, p.21-26, (1985).
20) T. Yamashita, G. L. Chen, J. Shir, and T. Chen: Sputtered ZrO2 Overcoat with Superior Corrosion Protection and Mechanical Performance in Thin Film Rigid Disk Application. *IEEE Trans. Magn.*, **21**, p.2629-2634 (1988).
21) B. Marchon, P. N. Vo, M. R. Khan, and J. W. Ager: Structure and Mechanical Properties of Hydrogenated Carbon Films Prepared by Magnetron Sputtering. *IEEE Trans. Magn.*, **27**, p.5160-5163 (1990).
22) T. Yamamoto, T. Toyoguchi, and F. Honda: Ultra-thin a-C:H Overcoats by pCVD on Thin Film Media. *IEEE Trans. Magn.*, **36**, p.115-119 (2000).
23) G. Marioto, F. L. Preire Jr, and C. A. Achete: Raman Spectroscopy on Nitrogen Incorporated Amorphous Hydrogenated Carbon Films. *Thin Solid Films*, **241**, p.255-259 (1994).
24) T. Toyoguchi, T. Yamamoto, and R. Koishi: Material and Tribological Properties of a-C:H Film by Plasma CVD for a Disk Overcoat. *IEEE Trans. Magn.*, **34**, p.1741-1743 (1998).
25) H. Hyodo, T. Yamamoto, and T. Toyoguchi: Properties of Tetrahedral Amorphous Carbon Film by FCA. *IEEE Trans. Magn.*, **37**, p.1789-1791 (2001).

**Takayuki Yamamoto** received the B.S. degree in Material Physics from Osaka University, Toyonaka, Japan in 1981 and the M.S. degree in Material Science from Toyota Technological Institute, Nagoya, Japan in 1987. He joined Fujitsu Laboratories Ltd. in 1981, where he was engaged in research and development of perpendicular magnetic recording. Since 1987, he has been engaged in research and development of tribology for head-disk interfaces. He is currently responsible for design and development of tribology for head-disk interfaces at Fujitsu Ltd.

**Yoshiharu Kasamatsu** received the B.S. degree in Industrial Chemistry from Nihon University, Narashino, Japan in 1989. He joined Fujitsu Laboratories Ltd. in 1989, where he was engaged in research and development of tribology for head-disk interfaces. He is now engaged in design and development of tribology for head-disk interfaces at Fujitsu Ltd.

**Hiroyuki Hyodo** received the B.S. degree in Material Engineering and the M.S. degree in Material Science from Tokyo Institute of Technology, Tokyo, Japan in 1994 and 1996, respectively. He joined Fujitsu Laboratories Ltd. in 1999, where he was engaged in research and development of fabrication processes for the carbon overcoats of magnetic media and magnetic heads. He is now engaged in research and development of fabrication processes for the PZT film of FRAMs.